

## RESULT

### Enhancing REServoirs in Urban development: smart wells and reservoir development, Geothermica Project Number 200317

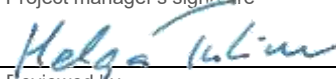


## RESULT-D6.5

### 3D Modelling of Lithology and Temperature in the Elliðaárdalur Low Temperature Geothermal Area, Reykjavík, SW-Iceland

Responsible authors:	Helga Margrét Helgadóttir, Arthurton Bellot and Gunnar Þorgilsson
Responsible WP-leader:	Helga Tulinius (WP6)
Contributions by:	



Report no. ÍSOR-2021/044	Date November 2021	Distribution <input checked="" type="checkbox"/> Open <input type="checkbox"/> Closed
Report name / Main and subheadings RESULT T-D6.5: 3D Modelling of Lithology and Temperature in the Elliðaárdalur Low Temperature Geothermal Area, Reykjavík, SW-Iceland		Number of copies 1
		Number of pages 31
Authors Helga Margrét Helgadóttir, Arthurton Bellot and Gunnar Þorgilsson		Project manager Helga Tulinius
Classification of report		Project no. 20-0115
Prepared for RESULT		
Cooperators OR		
Abstract Lithological logs from the Elliðaárdalur area in Reykjavík have been compiled from reports and simplified to build a geological model in the 3D software Leapfrog Geothermal. The stratigraphy in the area consists of interchanging basalt lava flows and hyaloclastite formations. Other relevant data, such as fractures and faults from geological maps and reports have been imported into the software. Fractures that have been mapped are mainly to the east of the Elliðaárdalur area but well data suggests that there are hydrological barriers both east and west of the main production area. These are thought to be faults with a similar orientation as most of the mapped fractures to the east. Temperature logs from the wells were synchronized and new temperature profiles created with linear interpolation in time for the years that were missing in between measured temperature logs. These logs were used to make a time dependent temperature model of the area. The resulting models provide a qualitative representation of the temperature changes in the system from 1968 to 2020. Just as the cold inflows are consistently in the south, the hot inflows dominate the northern and the central areas (at depth). Overall, the models show a gradual decrease in the system's temperature throughout the period.		
Key words Elliðaárdalur, geothermal, 3D modelling, Leapfrog Geothermal, geology, lithology, fractures, temperature, RESULT, ÍSOR, Iceland Geosurvey, OR		ISBN-number
		Project manager's signature 
		Reviewed by Sveinborg H. Gunnarsd., Kjartan Marteinson

## Table of Content

<b>1</b>	<b>Introduction .....</b>	<b>5</b>
<b>2</b>	<b>Geological model of the Elliðaárdalur geothermal area .....</b>	<b>6</b>
2.1	Surface data and well locations .....	6
2.2	Geological model .....	8
2.3	Tectonic structures in the area .....	13
2.4	Alteration.....	14
<b>3</b>	<b>Temperature model of the Elliðaárdalur geothermal area .....</b>	<b>16</b>
3.1	Methodology .....	16
3.2	Results of the temperature modelling .....	17
3.3	Discussion.....	26
3.4	Limitations of the temperature modelling .....	26
3.5	Conclusion from the temperature modelling .....	26
<b>4</b>	<b>Conclusions .....</b>	<b>27</b>
<b>5</b>	<b>References .....</b>	<b>28</b>
	<b>Appendix 1: List of data that has been imported in the 3D software from Seequent, Leapfrog Geothermal, that was used for both temperature and geological modelling .....</b>	<b>29</b>
	<b>Appendix 2: System block model and isosurfaces.....</b>	<b>30</b>

## Figures

Figure 1. <i>The Reykjavík capital area with the Elliðaárdalur geothermal area</i> .....	6
Figure 2. <i>Topography for the chosen area</i> .....	7
Figure 3. <i>Aerial photograph spread on topography with well locations and well traces</i> .....	7
Figure 4. <i>Aerial photograph of the Elliðaárdalur geothermal area and nearest surroundings</i> .....	8
Figure 5. <i>Well locations and lithological logs in the Elliðaárdalur geothermal area in Leapfrog Geothermal</i> .....	9
Figure 6. <i>Geological model of the extended Elliðaárdalur geothermal area</i> .....	10
Figure 7. <i>Lithological cross section ESE-WNW from the geological model</i> .....	11
Figure 8. <i>Lithological cross section N-S from the geological model</i> .....	12
Figure 9. <i>Lithology in wells and lithological cross sections from the model in 3D</i> .....	13
Figure 10. <i>Fractures and faults imported into Leapfrog Geothermal as well as hydrological barriers</i> .....	14
Figure 11. <i>First appearance of epidote in deep wells in the extended Elliðaárdalur geothermal area</i> .....	15
Figure 12. <i>First appearance of epidote in the wells shown with hydrological barriers</i> .....	16
Figure 13. <i>Distribution of available temperature logs in time in wells in the Elliðaárdalur field</i> .....	17
Figure 14. <i>3D view of the temperature model (1968)</i> .....	18
Figure 15. <i>Aerial view of a west-east cross section of the well cluster</i> .....	20
Figure 16. <i>Aerial view of a west-east cross section of the well cluster</i> .....	21
Figure 17. <i>Western view of isosurfaces 20°C and isosurfaces 100°C in 1968</i> .....	23
Figure 18. <i>Western view of isosurfaces 20°C and isosurfaces 100°C in 2018</i> .....	24
Figure 19. <i>Western view of cold isosurfaces and hot isosurfaces</i> .....	25

# 1 Introduction

In this report the intention is to describe both the geological model of the Elliðaárdalur geothermal area in Reykjavík (Figure 1), the capital of Iceland, as well as a separate time dependent temperature model. This report is part of the RESULT (Enhancing REServoirs in Urban deveLopmenT: smart wells and reservoir development, Geothermica Project Number 200317) project belonging to Work package 6 and is: D6.5: 3D modelling of lithology and temperature in the Elliðaárdalur low temperature geothermal area, Reykjavík, SW-Iceland.

Drilling in the Elliðaárdalur area started in 1967 and the last of the deeper wells (deeper than 500 m) was drilled in 1984. Several reports and studies have been made regarding the geology in the area and cuttings have been analysed in all the deeper wells. None of those cutting analyses were available in digital form. Therefore, considerable time was spent on gathering the data from reports and Figures. To start with, a report by Tómasson et al. (1977) was used to obtain rather detailed lithological logs from the oldest wells and more recent reports for the wells that were drilled in the 1980s and shallower wells drilled in the 1990s (Smáráson et al., 1984a, 1984b, 1985a, 1985b, 1988; Tulinius et al., 1986; Muhagaze, 1984; Tómasson, 1998a; Jónsson et al., 1998). The detailed logs are available as an excel file but have not been imported into a 3D modelling software. Scarce alteration information is also available in the excel file for potential use in the future. The geological model is described in Chapter 2.

In the last decades, a temperature decline has been observed in the Elliðaárdalur geothermal system. Cold water inflows attributed to a shallow aquifer was proposed as the basis for this loss in system temperature. To better understand the behaviour of the system, it was deemed necessary to create temperature models of the system throughout the time of well activity (~53 years). Temperature models were created using available downhole temperatures from the deeper wells in the Elliðaárdalur field, stored in the ÍSORs data base. The existing formation temperature and geological models were also provided as reference for this endeavour. The procedures and findings will be discussed in Chapter 3.

The 3D software from Seequent, Leapfrog Geothermal, was used for both temperature and geological modelling. A detailed list of data that has been imported into the software is in the Appendix 1.



**Figure 1.** The Reykjavík capital area with the Elliðaárdalur geothermal area marked specifically within the red rectangle. Aerial photograph from Google Earth.

## 2 Geological model of the Elliðaárdalur geothermal area

### 2.1 Surface data and well locations

To start with, a suitable area including the Elliðaárdalur geothermal area, and its surrounding was chosen and the topography for that specific area obtained from the National land survey of Iceland open database (Figure 2). Well locations (coordinates) and well traces were obtained from the ÍSOR database. The extended area was chosen on grounds of wells that were considered of interest regarding temperature, in case extended modelling would be done. The location of the wells can be seen in Figure 3 where most of the deeper wells are within the Elliðaárdalur geothermal area itself.

For clarification Figure 4 shows the Elliðaárdalur area within the red rectangle in Figure 1 along with the location of wells.

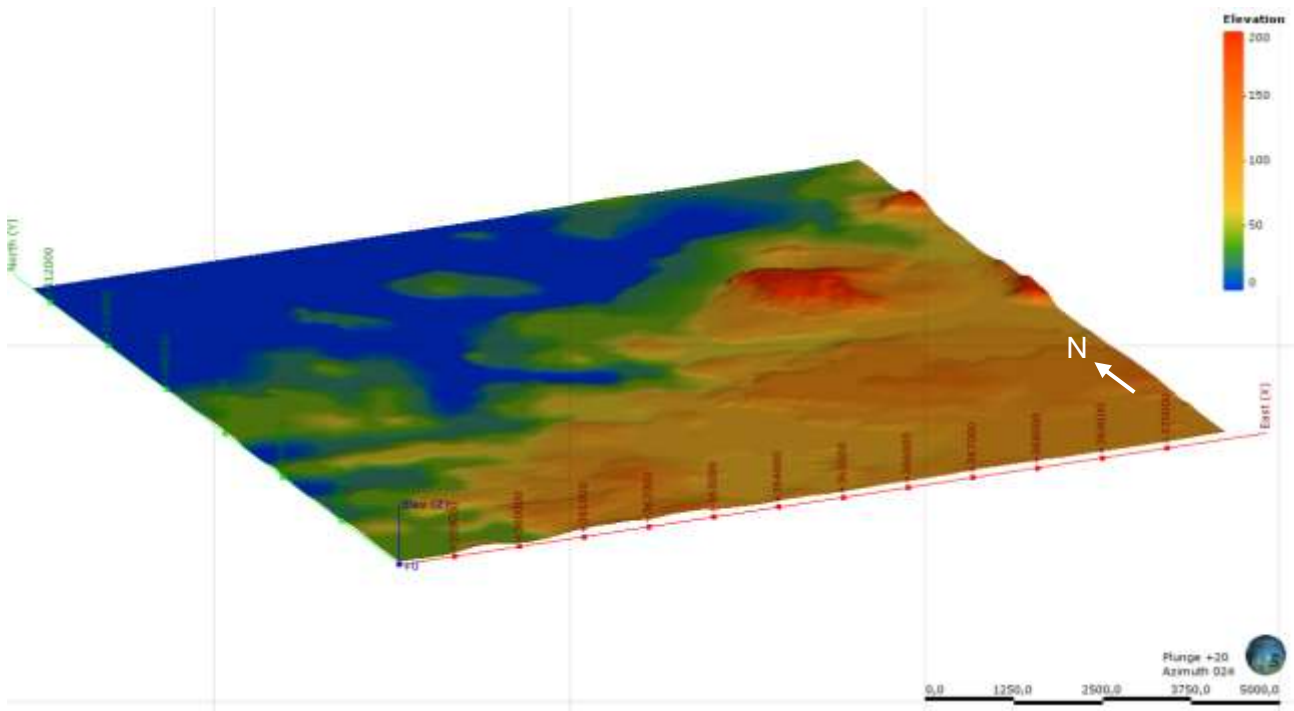


Figure 2. Topography for the chosen area. View from SSW.

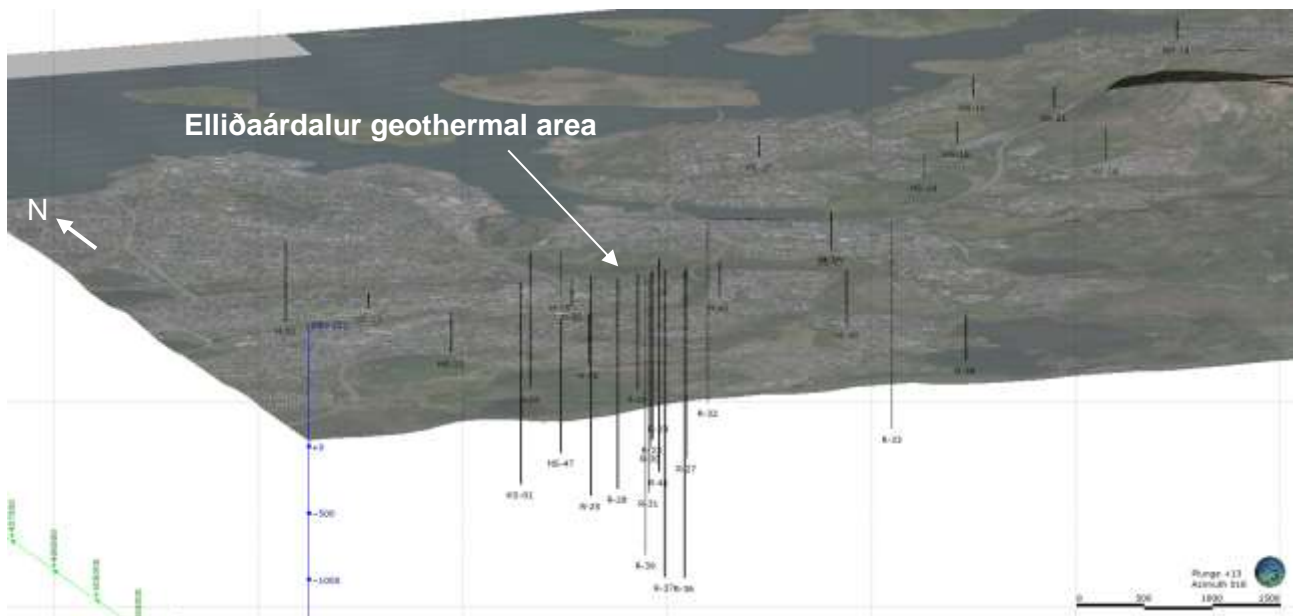
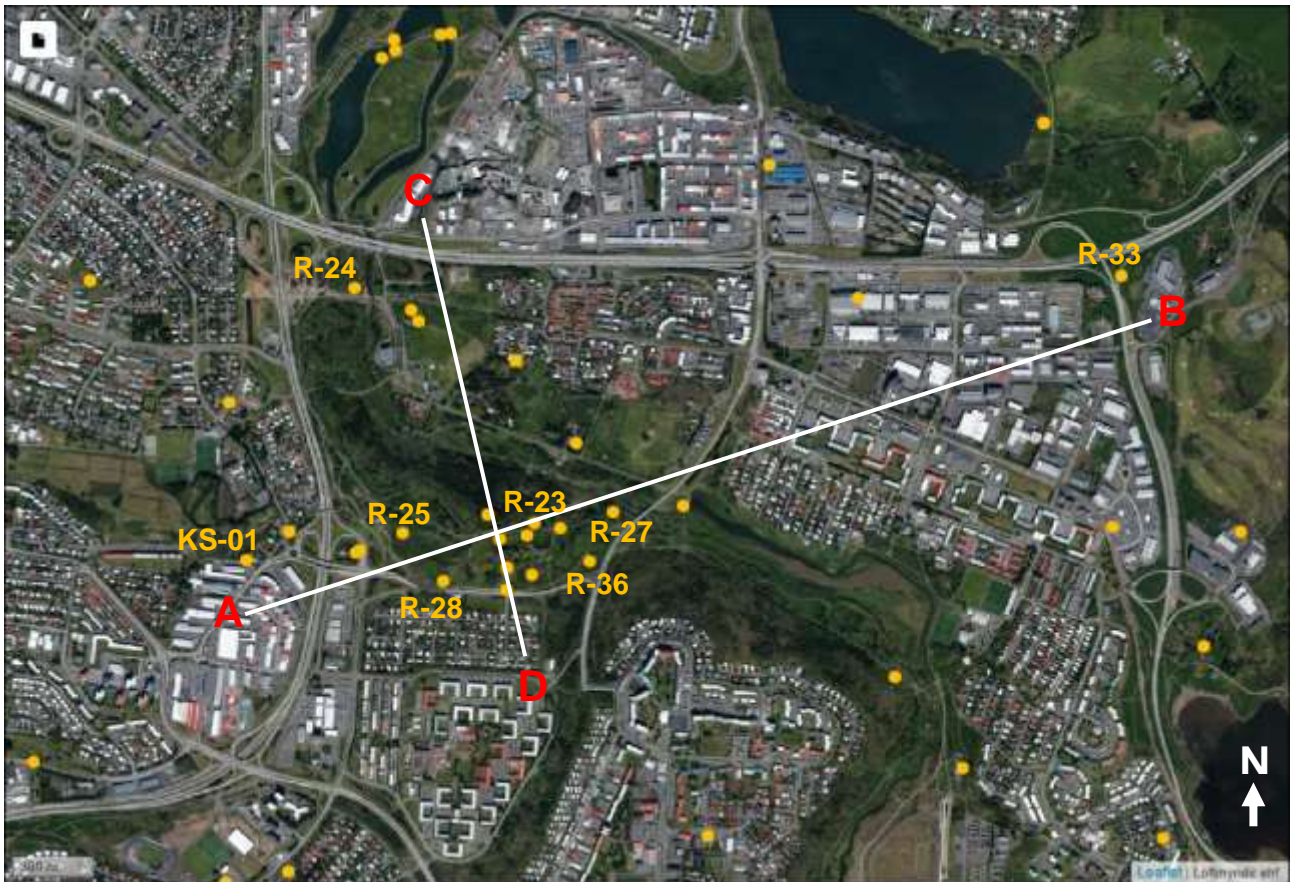


Figure 3. Aerial photograph spread on topography with well locations and well traces. View from SSW.



**Figure 4.** Aerial photograph of the Elliðaárdalur geothermal area and nearest surroundings. The cross-sections A-B and C-D are marked specifically as well as a selection of the wells for clarification. Yellow dots are wells, both shallow and deep.

## 2.2 Geological model

For the geological model the detailed logs from the deeper wells in the area were simplified and adjusted according to Tómasson (Tómasson et al., 1977; Tómasson, 1988, 1998b) with minor changes from the author of this report. The simplified logs were imported into Leapfrog Geothermal as the following formations: B-1, B-2, M-1, B-3, M-2, B-4, M-3, B-5, IS-1 and B-6. B-formations represent basalt lava flows, M-formations are hyaloclastite formations (including tuff, breccia and pillow basalts) and IS-1 is an intermediate formation found deep in the three deepest wells (R-36, R-37 and R-39). In general, the basalt lavas have formed during interglacial periods and the hyaloclastites during glacial periods. In addition, both intrusions from most wells and one thick sediment layer from one well were added to the lithological logs. The different formations are based on the reports by Tómasson et al. (1977) and Tómasson (1998b), in addition to formations from reports for the deepest wells (Smárason et al., 1984a, 1984b, 1985a, 1985b). The different formations were simplified even further in Tómasson (1988, 1990), dividing them into three units: **Upper basalts** (surface down to 350-400 m, including B-1 and B-2), **hyaloclastites** (from 350-400 m down to 950-1050 m, including M-1, B-3, M-2, B-4 and M-3) and **lower basalts** (below 950-1050 m down to about 1800 m).



Instead of using the simplest division of formations it was decided to make the lithological model in Leapfrog Geothermal using the original formations and adding the ones from the bottom of the deepest well, IS-1 and B-6 (Figure 5). Intrusions were noted specifically in the lithological logs for the wells but were not modelled specifically during this work. The intention is, if time permits, to work further on the geological model in the future, focusing on more details and the modelling of intrusive rocks, fractures and faults.

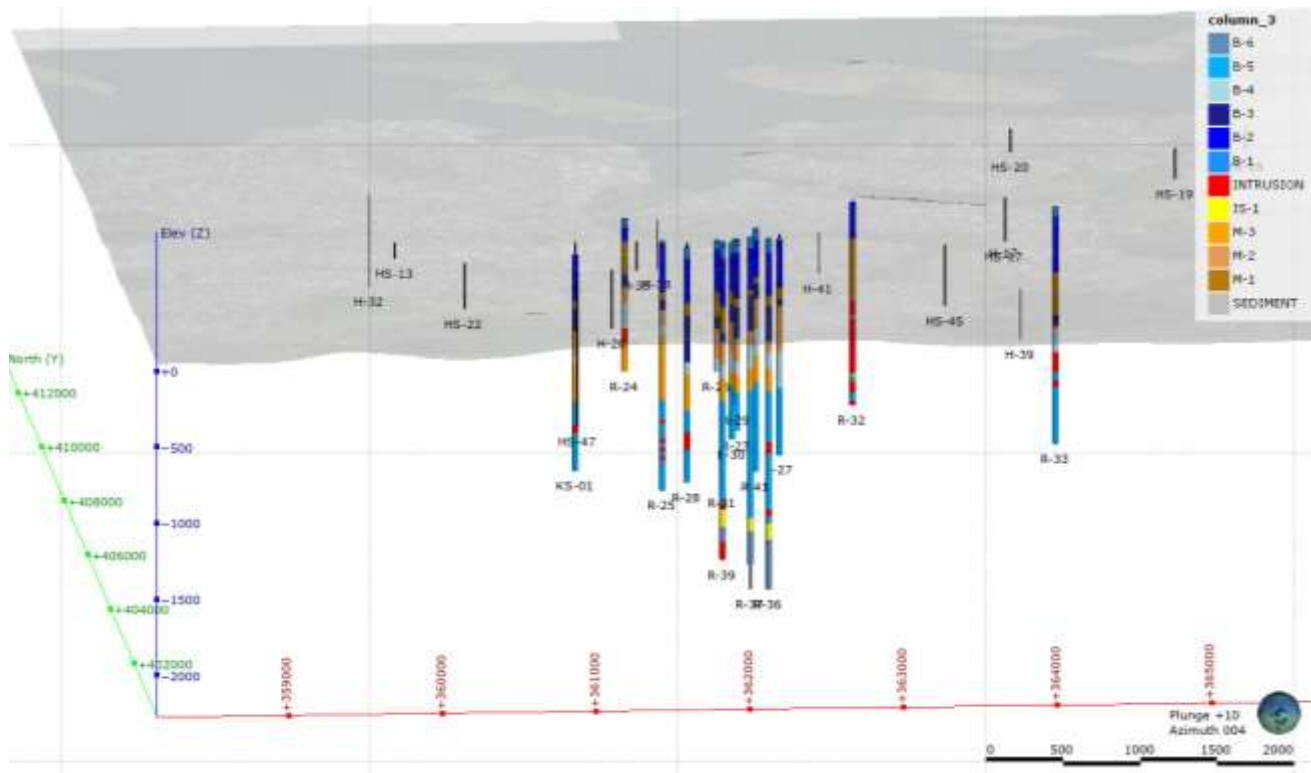


**Figure 5.** Well locations and lithological logs in the Elliðaárdalur geothermal area in Leapfrog Geothermal. View from south.

The geological model is shown in Figure 6. It is primarily built up of basalt lava flows with hyaloclastite formations dominating at around 350-400 m down to 950-1100 m depth. At around 1800 m depth intermediate rock has been logged in three of the deepest wells. The most densely drilled area, Elliðaárdalur area itself, is rather well known. The extended modelling to the east and northeast is more ambiguous, leaving large areas of uncertainty, especially at depth. Cross sections from the lithological model can be seen in Figure 7 and Figure 8. The density of wells in the immediate Elliðaárdalur area is apparent and the ambiguity of the area towards the outer margins of the model, especially at depth, is highlighted with a question mark. The cross sections with the wells in 3D are pictured in Figure 9. The simple division of formations into upper basalt, hyaloclastite and lower basalt (Tómasson, 1988) becomes rather distinct in the cross sections, highlighting the extensive glaciation in the area during the last glacial period with the hyaloclastite formations.

3D modelling of lithology and temperature in the Elliðaárdalur low temperature geothermal area, Reykjavik, SW-Iceland

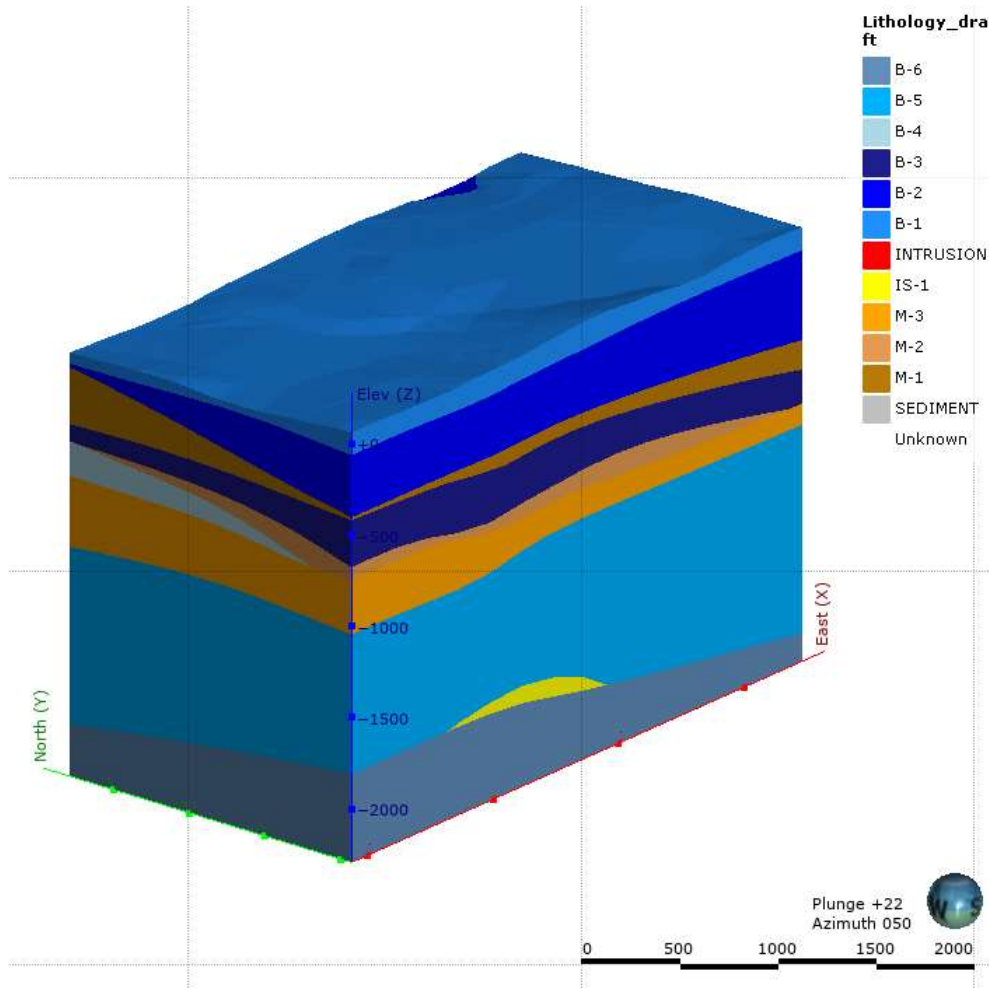
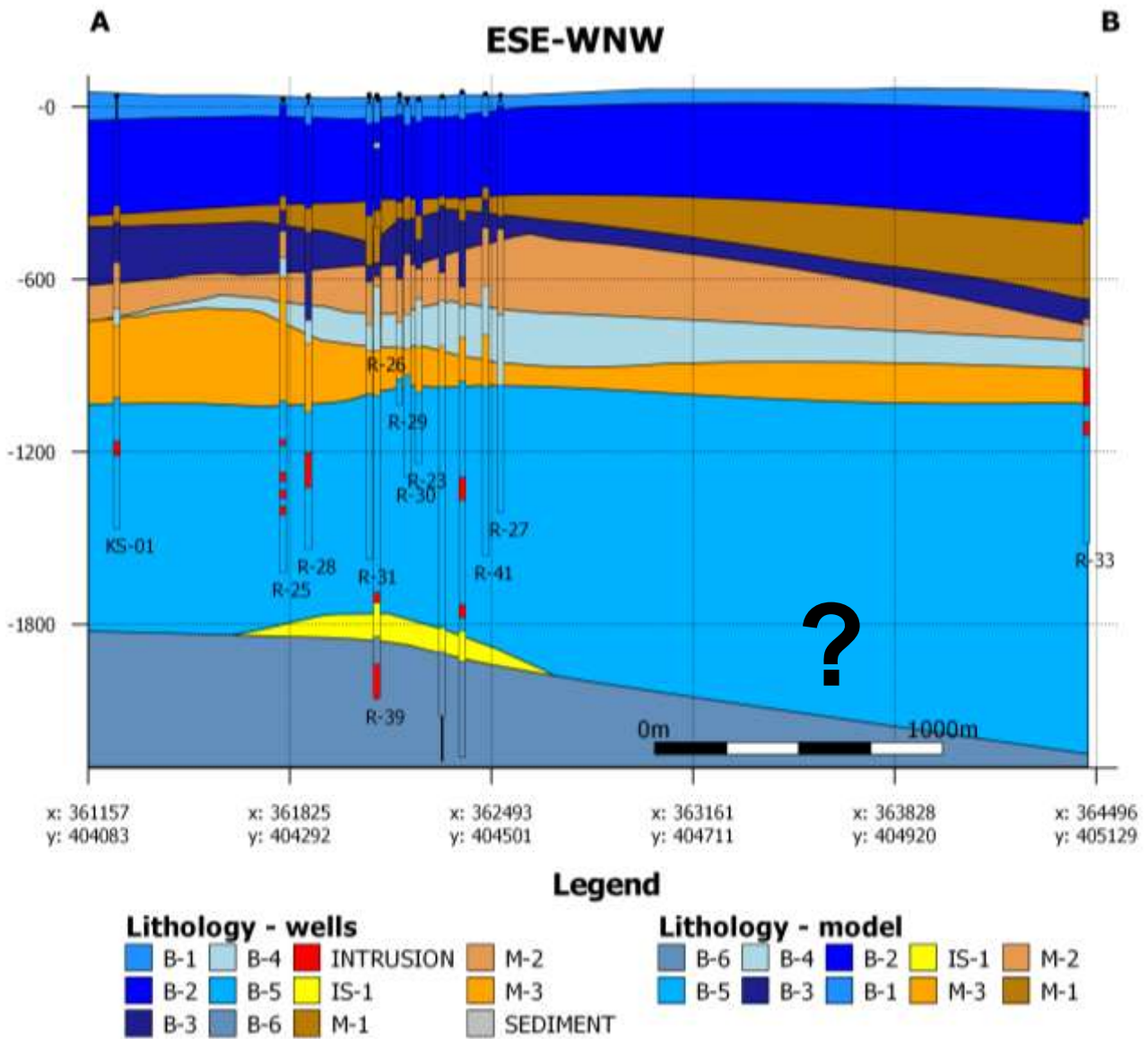
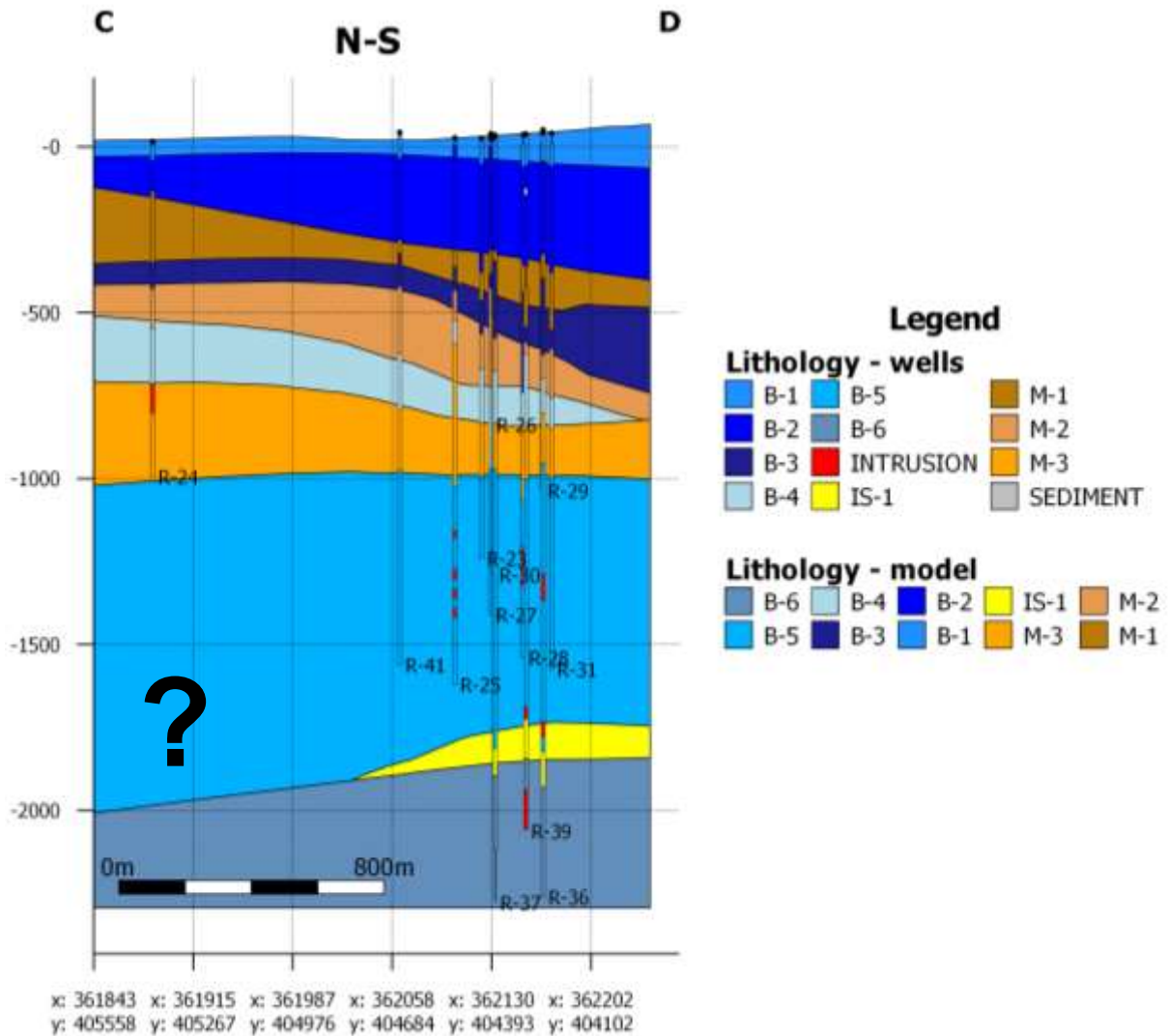


Figure 6. Geological model of the extended Elliðaárdalur geothermal area. View from WSW.



**Figure 7.** Lithological cross section ESE-WNW from the geological model. The location of the cross section is marked in Figure 4. Blue formations are basalt lava flows, brown/orange are hyaloclastite formations, yellow is intermediate rock.



**Figure 8.** Lithological cross section N-S from the geological model. The location of the cross section is marked in Figure 4. Blue formations are basalt lava flows, brown/orange are hyaloclastite formations, yellow is intermediate rock.

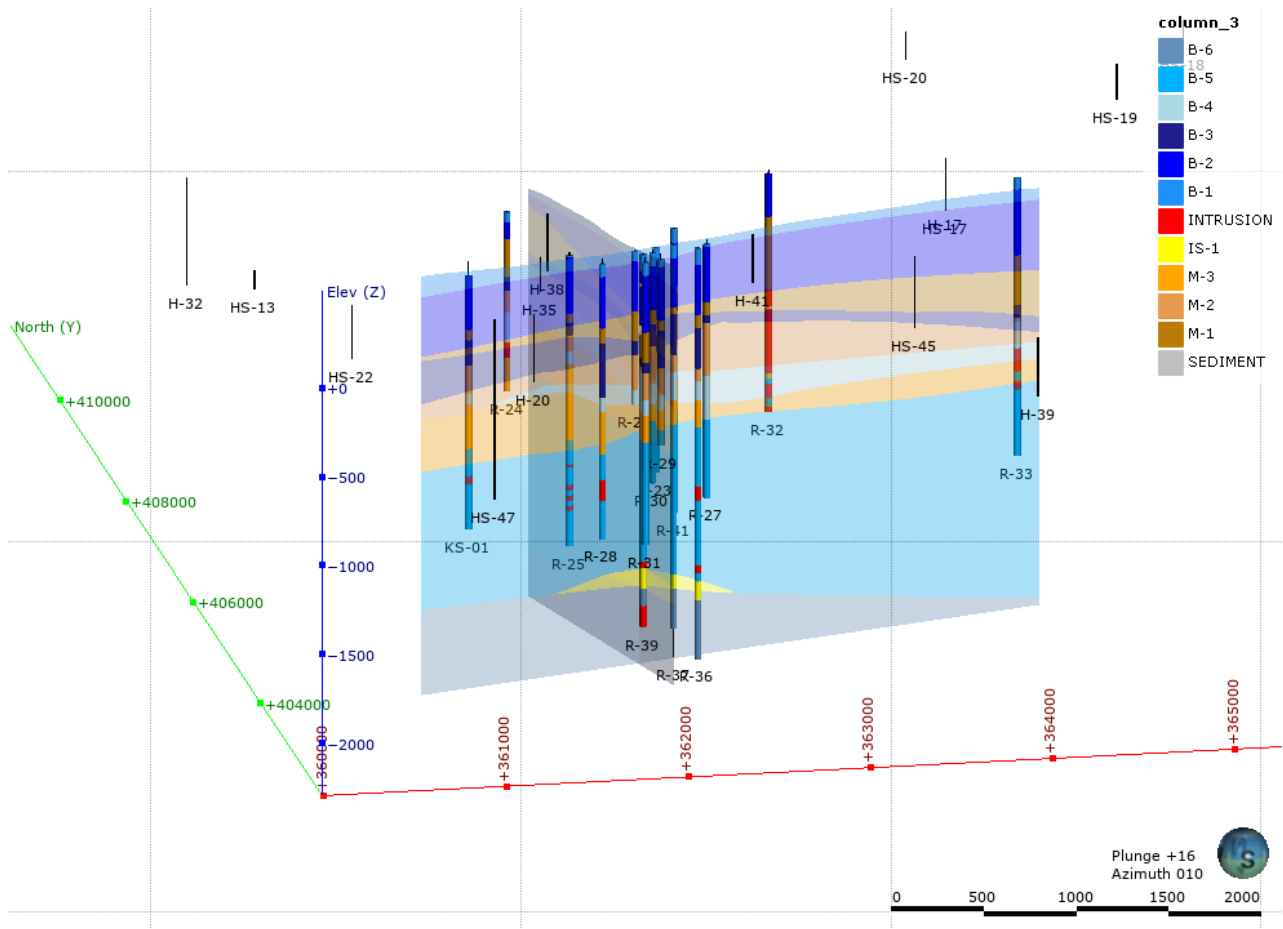


**Figure 9.** Lithology in wells and lithological cross sections from the model in 3D (see Figure 7 and Figure 8).

## 2.3 Tectonic structures in the area

Fractures from Sæmundsson et al. (2016) were imported into the software as well as fractures and possible fractures that have been published in a report by Torfason and Torfason (1991). None of these mapped fractures are in the immediate Elliðaárdalur area, but rather somewhat to the east. These fractures belong to the Krýsuvík fissure swarm. However, two features have been added to the model within the field, that are viewed as hydrological barriers, most likely faults. These barriers are based on hydrological evidence from the wells and mark the boundary of the production field to the west and east (Tómasson, 1988, 1990). These barriers have been traced on the topography of the area, in the software, using polylines and modelled as vertical meshes (Figure 10).

The fractures immediately to the east of the Elliðaárdalur area are dominantly NE-SW trending fractures belonging to the Krýsuvík fissure swarm. The hydrological barriers have a similar trend and are therefore likely to be connected to the fissure swarm. In addition, there are a few fractures that have been mapped that have a NW-SE trend, heading towards main production area. According to televiwer images from two wells (Helgadóttir, 2021) the open or partially open fractures linked to feed-points in the wells have a fracture trend of N-S to NE-SW as well as E-W and NW-SE. This difference in fracture trends from the mapped fractures highlights the importance of more detailed mapping of fractures in the area. It is well known that northerly striking transcurrent faults overprint

the NE-SW normal faults and fissures of the volcanic systems in the Reykjanes peninsula (e.g. Einarsson et al., 2020) but these have not been mapped in the immediate Elliðaárdalur area. Northerly striking lines were noted in the report by Torfason and Torfason (1991) and can be seen as both red and light green lines in Figure 10.

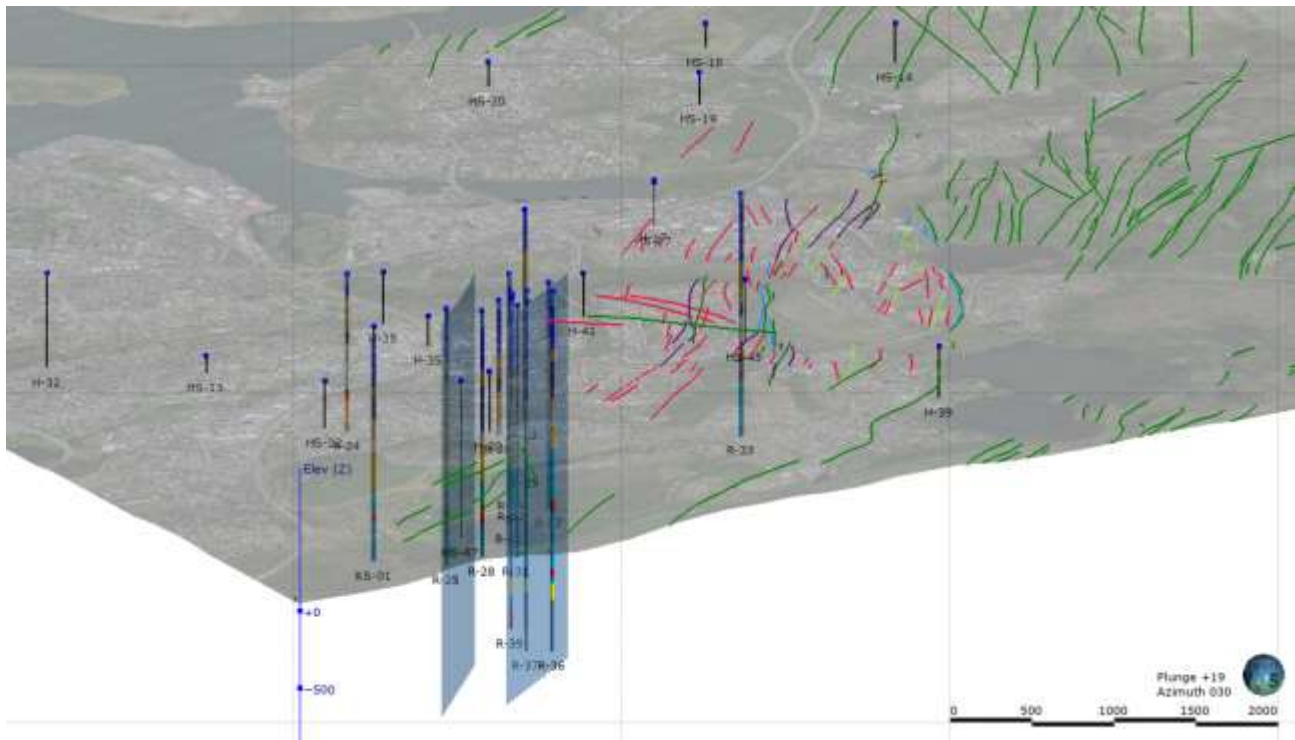


**Figure 10.** Fractures and faults imported into Leapfrog Geothermal as well as hydrological barriers (possible faults) from well data within the main geothermal area. View from south southwest. Dark green lines: Fractures and faults from Sæmundsson et al. (2016). Light blue lines: faults; purple lines: probable fractures; light green lines: ambiguous fractures, red lines: lines that may be fractures (Torfason and Torfason, 1990). Hydrological barriers modelled as vertical walls from polylines drawn from Tómasson (1988).

## 2.4 Alteration

Available alteration data is very limited. The first appearance of epidote is, however, noted in several wells and has been imported into the model (Figure 11). Epidote alteration in the wells suggests that temperature in the area used to be much higher than it is today where zeolites surely overprint the fossil signs of the peak of the geothermal system. It is interesting that the depth to the first appearance of epidote is much shallower within the production area, in between the hydrological barriers that have been suggested from well data (Figure 12). This implies that the barriers have most likely existed for some time, at least since the peak of the geothermal activity. Other alteration data is scarce and has not been imported into Leapfrog.

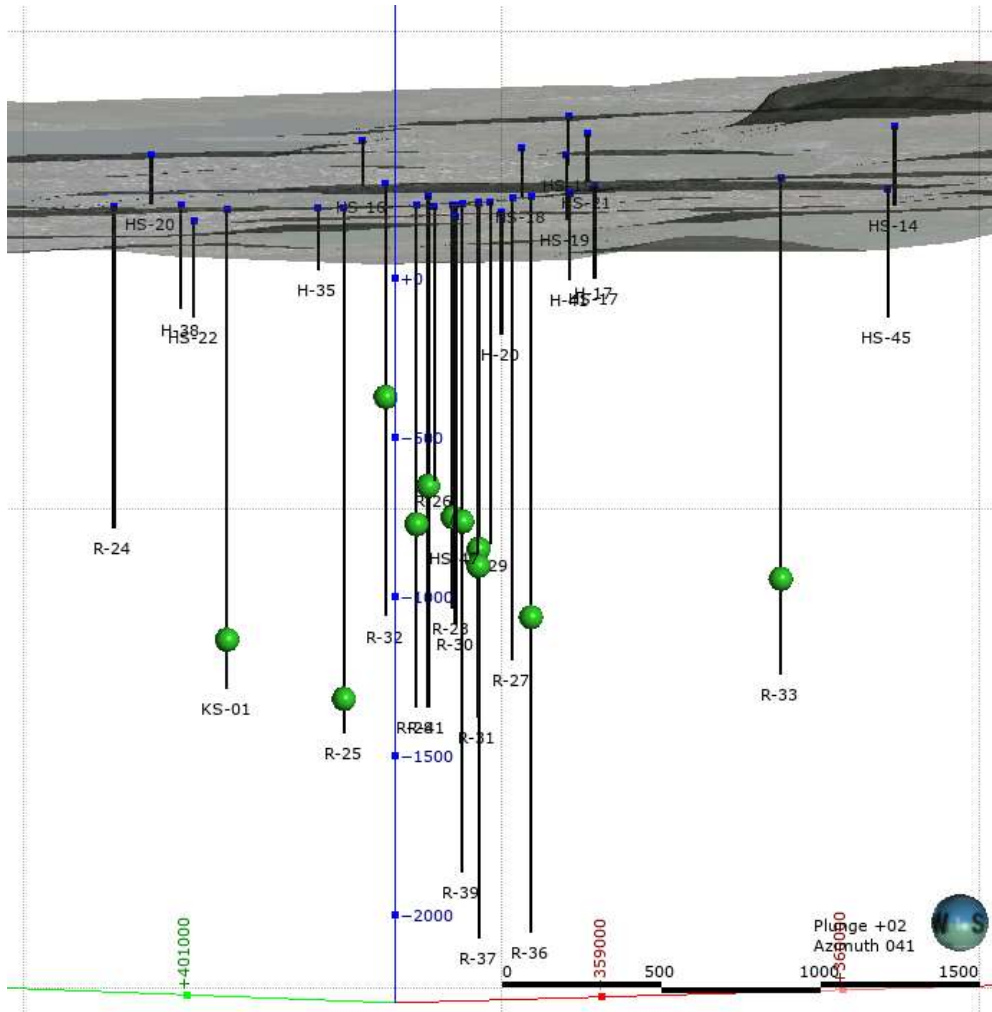


**Figure 11.** First appearance of epidote in deep wells in the extended Elliðaárdalur geothermal area. Epidote alteration suggests that temperature in the area used to be much higher in the past than it is today. View from southwest.

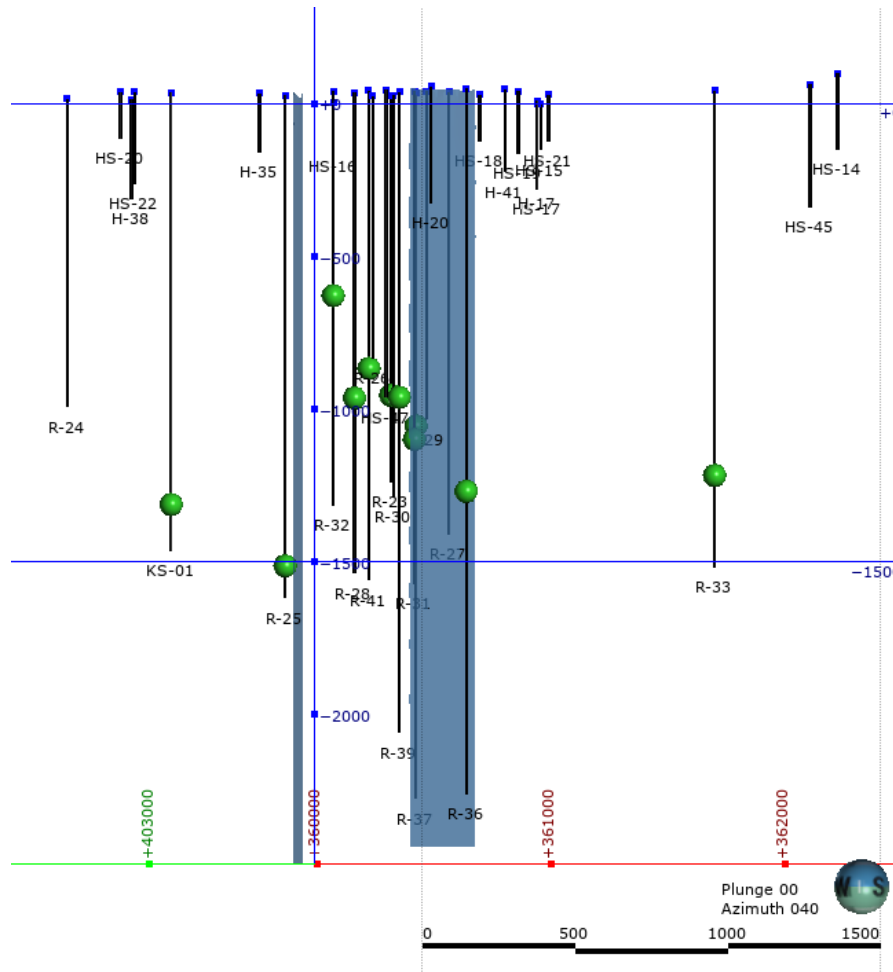


Figure 12. First appearance of epidote in the wells shown with hydrological barriers (bluish grey planes to the right of R-25 and to the left of R-36).

### 3 Temperature model of the Elliðaárdalur geothermal area

#### 3.1 Methodology

##### 3.1.1 Well Data

The well coordinate data was provided with the geological model. All available downhole temperature logs for wells R-26, R-41, R-37, R-28, R-27, R-24, R-25, KS-01, R-29, R-30, R-39, R-23, and R-31 were retrieved from the ÍSOR in-house database. Each well often has several logs per year, measured with the well in various conditions, that do not represent the well at equilibrium conditions. The distribution of available temperature logs in time is shown in Figure 13.

For simplicity the last temperature log of each year was chosen to represent the downhole temperature of the well. The chosen set of temperature logs were then resampled in depth with linear interpolation synchronizing the depth values of the temperature logs between wells. From the synchronized logs new temperature profiles were created, with linear interpolation in time, for the years that were missing in between measured temperature logs.



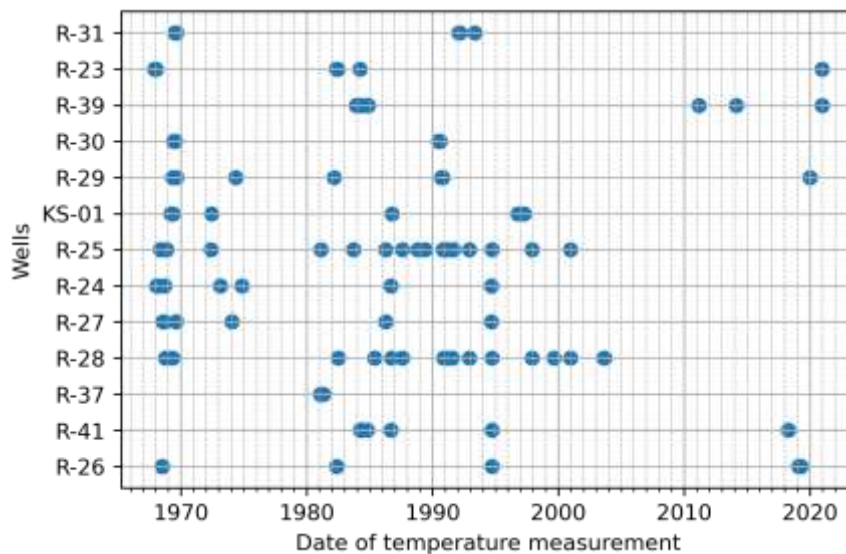


**Figure 13.** Distribution of available temperature logs in time in wells in the Elliðaárdalur field.

The downhole temperatures recorded in those wells were then added after compiling the temperature recordings of each well into master files for each available year. This information was imported as data points into Leapfrog Geothermal and served as the basis for creating the following numeric models.

### 3.1.2 Defining the Temperature Models

The temperature models were created using the **Numeric Model** function within Leapfrog Geothermal. A radial basic function (RBF) interpolation was utilized for each year separately resulting in a total of 53 models. The boundaries for these models were created initially from the boundary of the existing geological model and was then reduced to focus on the well data that was provided. It was then necessary to select the range for the isosurfaces which are used to define the temperature models (see Appendix 2). A range of discrete values from  $< 20^{\circ}\text{C}$  to  $> 100^{\circ}\text{C}$ , at  $20^{\circ}\text{C}$  intervals, was used resulting in 6 isosurfaces. This range was taken from the existing formation temperature model. An additional 53 temperature models were created using the temperature profiles without casing temperatures. These profiles, though obviously different quantitatively, do not display a significant difference when compared qualitatively throughout the entirety of the models. The difference is most significant around the wells. This can be attributed to the fact that the provided data is focused on the wells and not the wider area. A block model was also created for the system (see Appendix 2). This can be used for further numerical analysis of the system.

## 3.2 Results of the temperature modelling

The resulting temperature models provided a qualitative representation of temperature distribution in the specified section of the system. As seen in Figure 14, the orange and red sections at the top of the model correspond to the location of the well cluster. As such, the data at this point (and at the depths beneath) provides the most accurate part in this model in contrast to the less refined areas nearer to the boundaries.

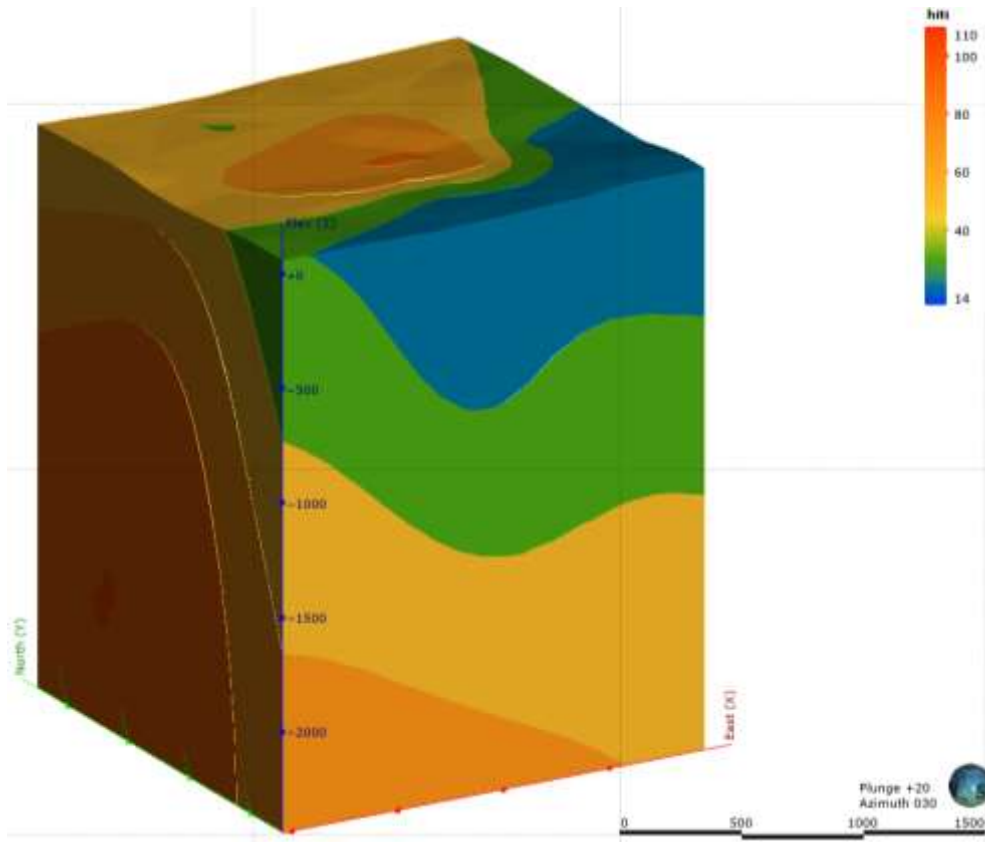


**Figure 14.** 3D view of the temperature model (1968). The colour scale indicate temperature (blue > 20°C green 20°-40°C, yellow 40°- 60°, light orange 60°-80° and dark yellow 80 – 100°C).

A depth range of 700 m – 1100 m was chosen as the area of focus for this study to encompass an area closer to the general production zone of the wells. Figure 15 and Figure 16 (Table 1) display the top of this depth range at 700 m depth. An interval of 5 years was used to show the temperature changes from 1968 to 2020 with the final interval consisting of 8 years (2013-2020). The first model of each interval was used, in addition to the distribution of 2020.

**Table 1**

Figure 15		Figure 16	
1	1968	1	1993
2	1973	2	1998
3	1978	3	2003
4	1983	4	2008
5	1988	5	2020

Wells R-23 through R-28 provided the downhole temperature data for the year 1968. Considerably colder temperatures can be observed to the south of the model with warmer temperatures situated

around the wells in the centre and to the north of the model (Figure 15 – upper left). This cold zone appears to be the result of a lack of data in the wider model as temperatures increase significantly throughout the model in the following year with the addition of temperature data from newly drilled wells R-29 through R-32 and KS-01. The resulting distribution no longer has this extremely cold zone and displayed an area of more than 100°C around wells R-23, R-26, R-29, and R-30. Well R-33 was also drilled within this period (1971); however, this well sits outside the boundary of this model and did not affect the model's temperatures.

At the start of the second interval (1973 – 1977), no new wells have been added, however a shift in the temperature distribution can be observed. In the model for the year 1973, the northern and eastern sections dominate the model as the hottest sections while a cooler zone can be observed in the south west, appearing to move towards the well cluster (Figure 15 – upper right). Like for the previous interval, there is an increase in the system's temperature in the following year which gradually decreases towards the end of the interval.

The next interval starts 1978 and it can be observed that the temperature distribution resembles the distribution of 1973 (Figure 15 – middle left). Unlike the previous two intervals, a temperature increase was not observed in the following years. The cold front coming from the south west section is moving north, reaching well R-28. The wells added during this period were R-36, R-37, and R-39.

For the next 5 years the cold front in the south-west gradually expands to the south-east, see. Figure 15 (middle right) and t Figure 15 (bottom). The direction of this cold front follows the trend set by the SW-NE trending fault which could be acting as a conduit directing the cold inflows from the southwest quadrant towards the centre of the model. The entire system's temperature has also dropped because of this growing cold front, and the temperatures of wells R-29 and R-36 have permanently dropped below 80°C.

The growing cold front observed in the previous two intervals disappears in 1991, probably do to new deeper casing in some of the wells and is replaced by warmer temperatures observed in the south of the model in Figure 16 (upper left). The disappearance of this cold zone has contributed to an overall increase in the system's temperature. The hottest zones are situated around the wells, generally towards the north and northeast of the model.

During the next interval (1998 – 2002), colder temperatures return to the model, this time from the south eastern quadrant as shown in Figure 16 (upper right). This could represent a cold-water zone situated further south, outside of the model's extents. This cold-water zone would have contributed to the cold front observed in previous intervals, with the SE-NW trending fault acting as the conduit. In the following interval (2003 – 2007), the cold front in the southwest reappears, contributing to a significant temperature loss in the western section of the model (Figure 16 – middle left). With the temperatures in the southeast remaining low the average temperature of the entire system decreases as a result.

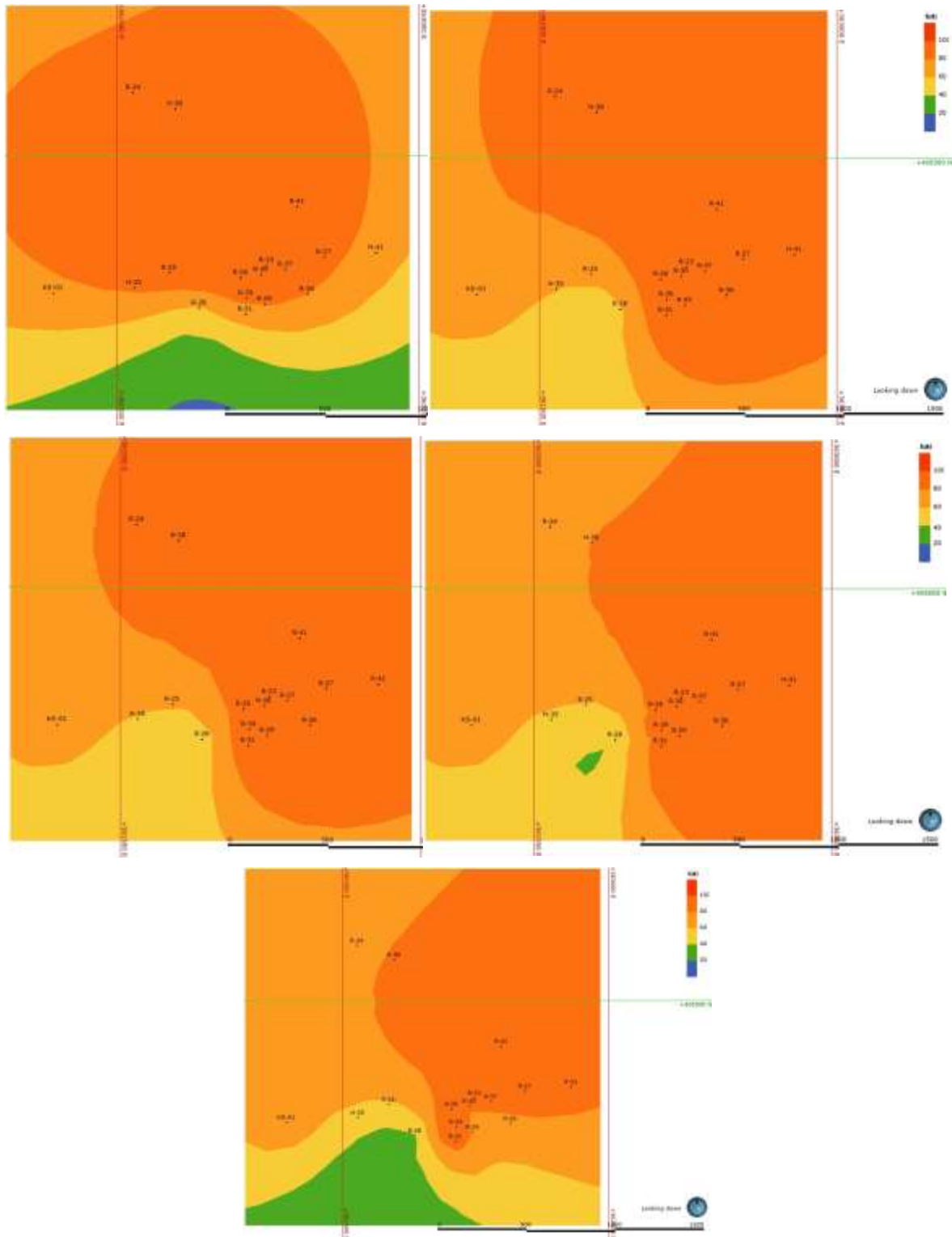


**Figure 15.** Aerial view of a west-east cross section of the well cluster showing the downhole temperatures recorded at 700 m depth in 1968 (upper left), 1973 (upper right), 1978 (middle left), 1983 (middle right) and 1988 (bottom). The colour scale indicate temperature (blue > 20°C green 20°-40°C, yellow 40°- 60°, light orange 60°-80° and dark orange 80 – 100°C).

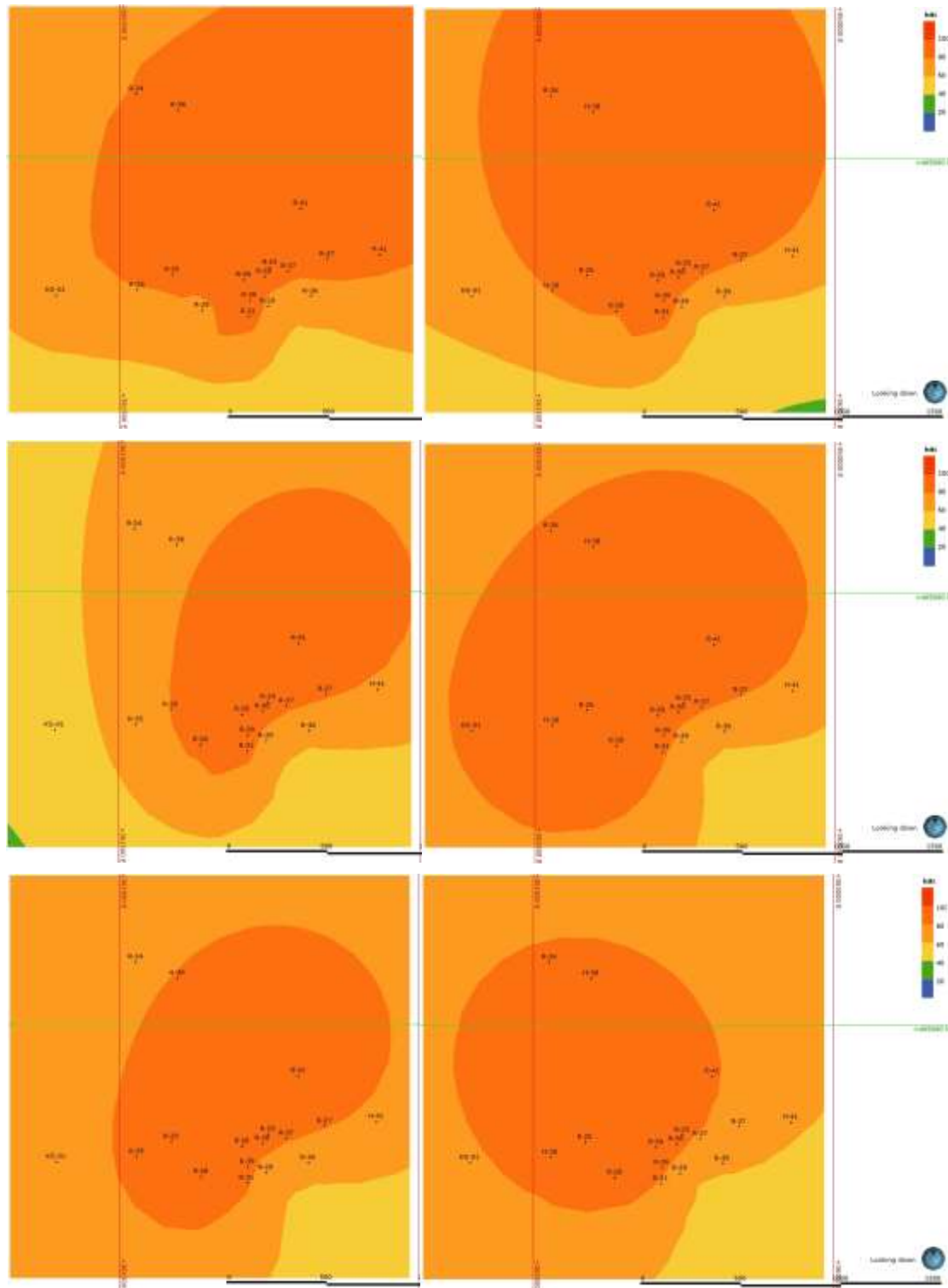


**Figure 16.** Aerial view of a west-east cross section of the well cluster showing the downhole temperatures recorded at 700 m depth in 1993 (upper left), 1998 (upper right), 2003 (middle left), 2008 (middle right), 2013 (bottom left) and 2020 (bottom right). The colour scale indicate temperature (blue > 20°C, green 20°-40°C, yellow 40°- 60°, light orange 60°-80° and dark yellow 80 – 100°C).

Figure 16 (middle right) represents the temperature distribution in 2008 at the beginning of the 9<sup>th</sup> interval (2008 – 2012). The model displays an increase in the overall system's temperature with most of the wells situated within the 80°C- 100°C range. The warm zone in the southeast remains present in the model and will remain until the end of the study period.

The temperatures observed in the final interval (2013 – 2020) is generally hot, as shown in Figure 16 (bottom left). By the end of the period in 2020, the temperatures have remained generally hot, with the warm zone in the southeast slightly expanding (Figure 16 – bottom right). The hottest temperatures are in the centre of the model, encompassing most of the wells.

Throughout the previously discussed intervals, the model has shown various fluctuations in temperature. Figure 17 displays the temperature isosurfaces for 20°C and 100°C at the start of the production period (in 1968) Figure 18 shows the same temperature isosurfaces in 2018, when the last isotherm of 100°C was recorded. In 1968, it can be clearly observed that there was a significant hot zone dominating the model centre and north-western sections, with a small cold zone in the southeast section of the model at ~750 m depth. This hot zone signifies a major hot inflow in the system while the cold zone depicts a minor cold-water inflow. In 2018, however, these two zones have dramatically decreased, especially the hottest temperatures which are isolated to a very small section deep in the centre of the model. Though the model may have been drastically impacted by a lack of well data in earlier years, there is still an indication of a significant drop in temperature throughout the model since the start of production.

Figure 19 displays the constant cold and hot isosurfaces observed throughout the 53-year period. Colder temperatures are originating from the south at a maximum depth of ~ 750 m, trending towards the centre of the model (at albeit much shallower depths). The hottest temperatures are in the centre of the model (as shallow as ~200 m depth) and the northern section (as shallow as ~1500 m depth). This consistent placement of these isotherms might have significant implications on future drilling prospects in this geothermal system.

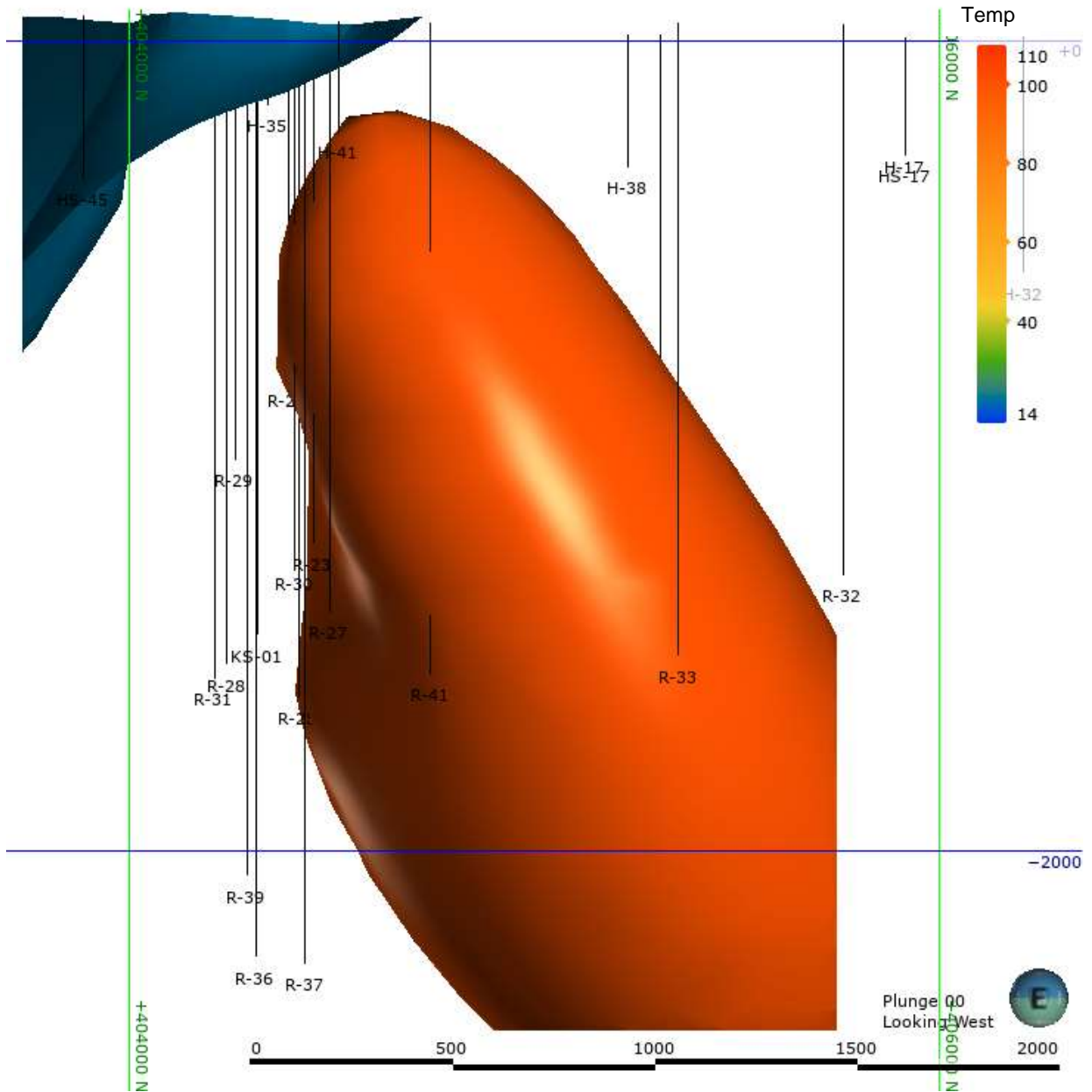


Figure 17. Western view of isosurfaces 20°C (dark green/blue) and isosurfaces 100°C (dark orange/red) in 1968.

3D modelling of lithology and temperature in the Elliðaárdalur low temperature geothermal area, Reykjavík, SW-Iceland

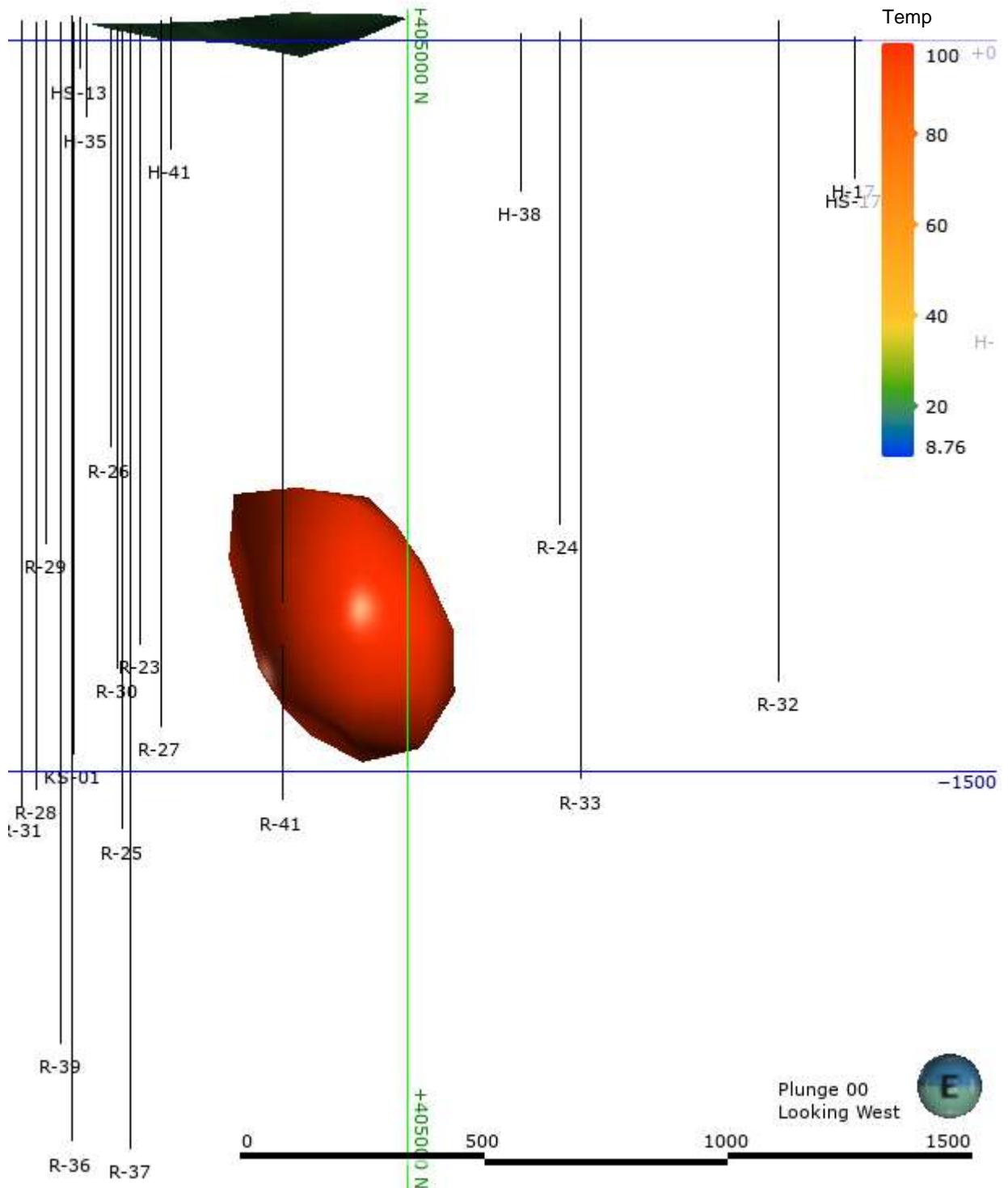


Figure 18. Western view of isosurfaces 20°C (dark green/blue) and isosurfaces 100°C (dark orange/red) in 2018.



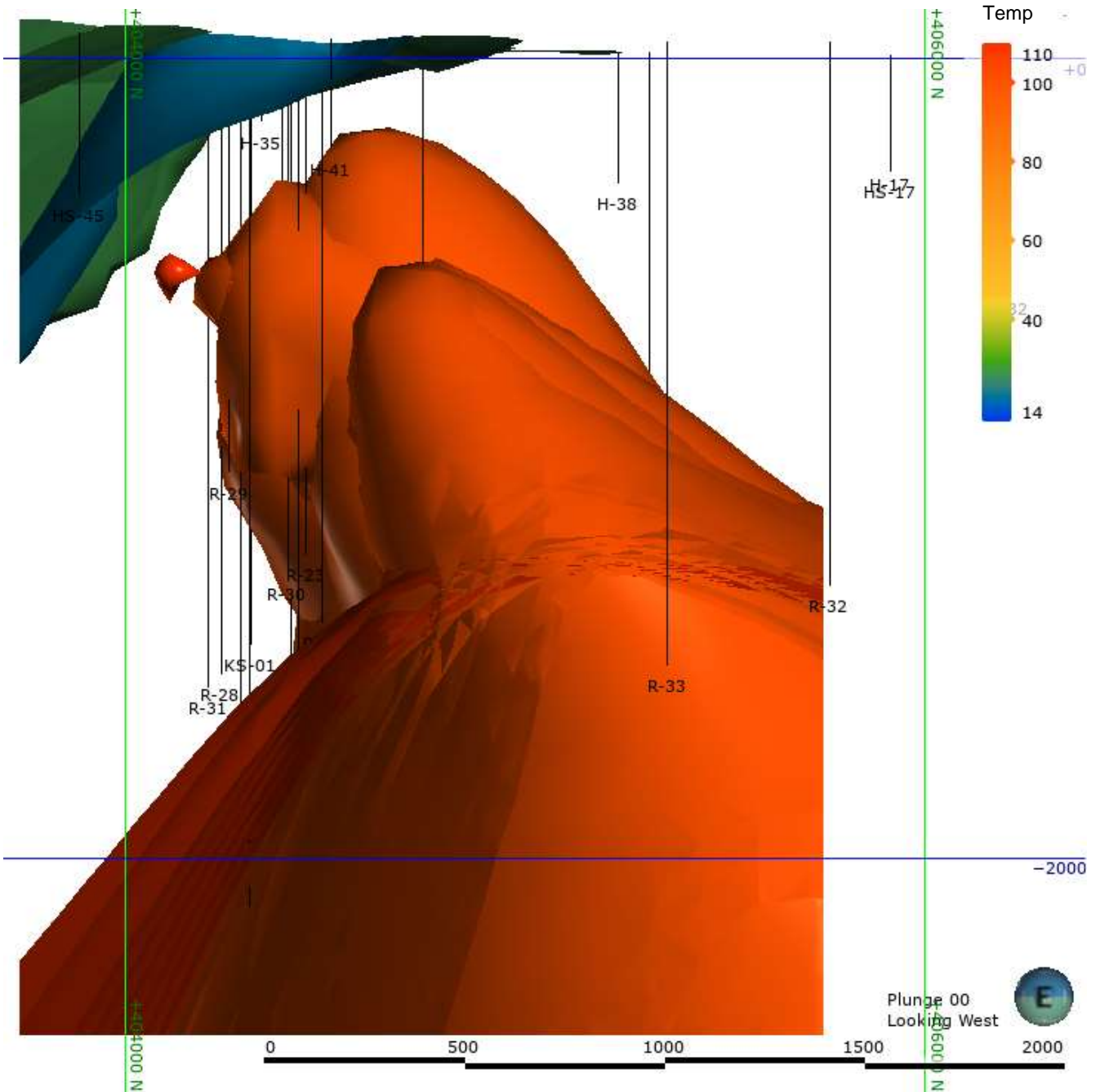


Figure 19. Western view of cold isosurfaces (blue/green) and hot isosurfaces (dark orange/red).

### 3.3 Discussion

The earlier temperature models suggest a dominating cold zone (i.e., aquifer) to the south and south-west of the model. Circulation losses were mainly observed at the M-2/B-4 lithological boundary with additional losses observed at the M-3/B-5 and B-4/M-3 boundaries. The aquifer was observed at max depth ~ -750 m; an unusually deep zone for a cold-water reservoir.

Three major inflow zones have been observed:

- 1969-1994: possibly originating from the SW quadrant, through the SW-NE fracture zone towards the centre of the model.
- 1995-2003: possibly originating from the south, predominantly through the SW-NE fracture zone towards the centre of the model.
- 2004-2019: focused predominantly at very shallow depths in the centre of the system. It is possible that this inflow is the result of the previous two inflows coming in through cracks formed by reinjection over time.

It was observed in previous reports that the temperatures beneath the casing of R-29 is colder than the observations in the nearby wells. Though this was also represented in the models, the cause for this has not yet been found.

### 3.4 Limitations of the temperature modelling

There is only one temperature log for the year 1967. As such, Leapfrog Geothermal did not have the capacity to extrapolate enough information to create a useful temperature model for that year.

As previously mentioned, the temperature models are focused on the wells that provided the required data. This causes uncertainty in the temperature distribution of the models away from the centre where the well cluster is found. Additionally, the model boundaries also create some inconsistencies in the temperature distribution (e.g. the drastic temperature shift between 1968-1969). This can be rectified by defining the appropriate boundary conditions when creating a numerical flow model, which could be one of the next steps of this project.

### 3.5 Conclusion from the temperature modelling

The resulting models provide a qualitative representation of the temperature changes in the Elliðaárdalur geothermal system. Three major inflow zones have been observed (1969-1994, 1995-2003 & 2004-2019). The temperature information suggests that these inflows are connected to an aquifer dominating the southern section of the system. This aquifer is unusually deep considering how low these temperatures appear. The SE – NW and more predominantly SW – NE fracture zones appear to have provided a pathway for this cold-water to be directed towards the well cluster in the centre of the system, though the cold-water temperatures are at much shallower depths towards the centre of the model. Just as the cold inflows are consistently in the south, the hot inflows dominate the northern and the central areas (at depth). Overall, the models have shown a gradual decrease in the system's temperature throughout the period and though the temperatures in 2020 are generally hot, the high temperatures observed in earlier years are no longer present. This appears to be the result of the cold southern inflows impacting the system, combined with the production history of the system. It should be noted, however, that due to the amassed data around the wells, the temperature information is more accurate towards the centre and this could give a misleading representation of the temperature models.

## 4 Conclusions

These two models introduced in this report will be used for further work on understanding the Elliðaárdalur geothermal field. Dikes and other geological features will be added and the relationship between geology and feed zones can be studied. By reducing the temperature intervals more features can come to light in the temperature model. The temperature model of the system indicates that there might be a cold water aquifer at depth in the south of the field. Inflow from this aquifer seems to contribute to the overall cooling of the system over its production lifetime. The temperature modelling could be expanded by creating a numerical flow model for the system. Such a model would be useful in helping to predict the future temperature evolution of the field.

## 5 References

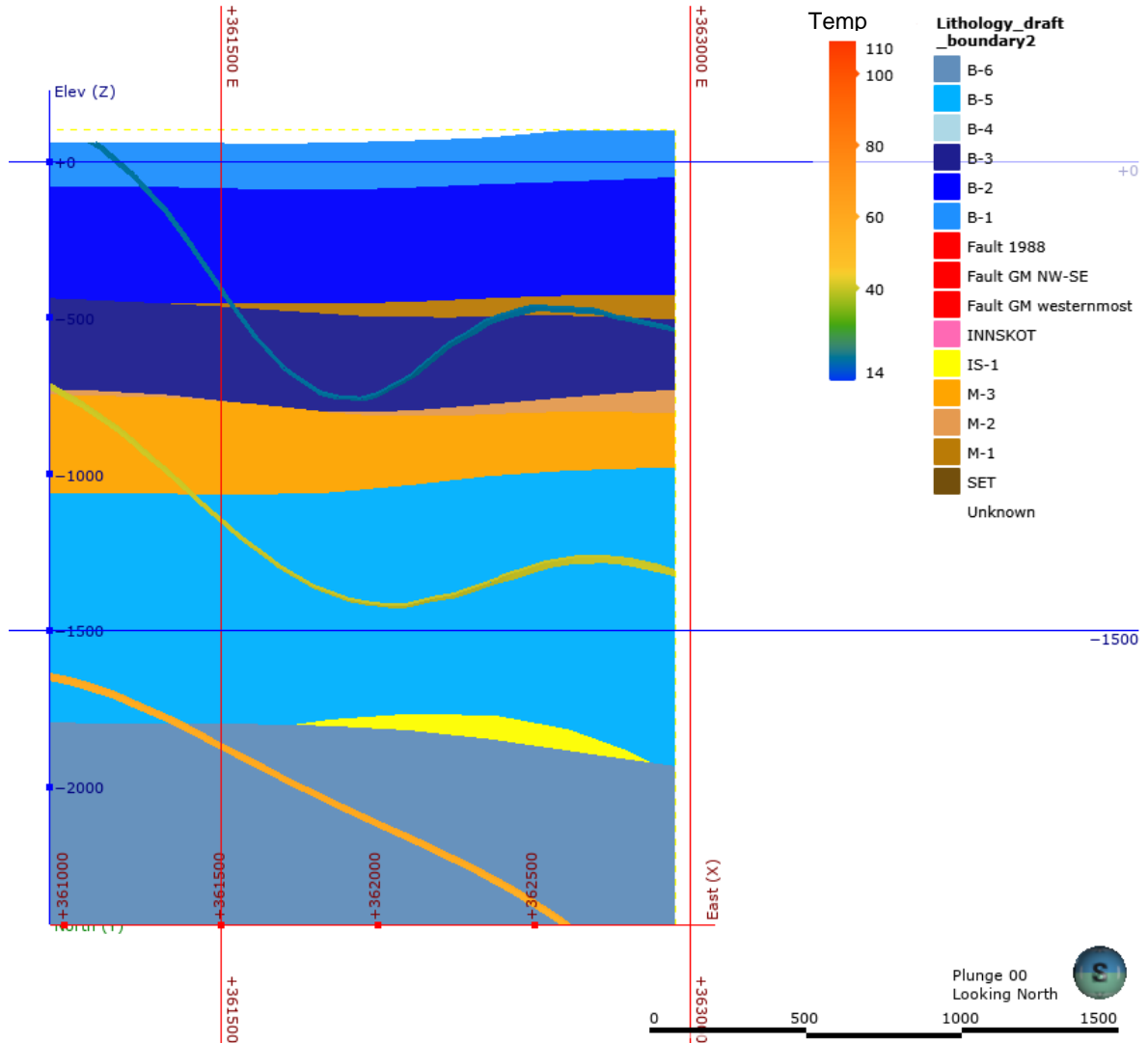
- Einarsson, P., Hjartardóttir, Á.R., Hreinsdóttir, S. and Imsland, P. (2020). The structure of seismogenic strike-slip faults in the eastern part of the Reykjanes Peninsula Oblique Rift, SW Iceland. *Journal of Volcanology and Geothermal Research* 391, 11 p.
- Helgadóttir, H.M. (2021). *RESULT T-D6.4: Results of Borehole Televiewer Logging in Wells R-23 and R-39 in Elliðaárdalur, Reykjavík*. Iceland Geosurvey, ÍSOR-2021/025, 60 pp. + Appendices.
- Jónsson, S.S., Guðlaugsson, S.P., Friðleifsson, G.Ó., Tulinius, H. and Steingrímsson, B. (1998). *Höfuðborgarsvæði. Holur HS-45 til HS-48. Jarðfræði og jarðlagamælingar*. National Energy Authority report. In Icelandic. OS-98015, 41 pp.
- Muhagaze, L. (1984). *Geological mapping and borehole geology in geothermal exploration*. United National University. National Energy Authority, 38 pp.
- Smárason, Ó.B., Tulinius, H., Hermannsson, G., Thorsteinsson, Þ., Tómasson, J. and Harðardóttir, V. (1988). *Reykjavík, hola RV-41. Borholurannsóknir*. National Energy Authority report. In Icelandic. OS-88026/JHD-02, 59 pp.
- Smárason, Ó.B., Tulinius, H., Tómasson, J., Hermannsson, G., Ágústsson, H. and Benediktsson, S. (1984a). *Reykjavík. Hola RV-39. Borun fyrir 13½" fóðringu*. National Energy Authority report. In Icelandic. OS-84036/JHD-11, 21 pp.
- Smárason, Ó.B., Tulinius, H., Tómasson, J., Thorsteinsson, Þ., Gunnlaugsson, E., Hermannsson, G. and Ágústsson, H. (1984b). *Reykjavík – Hola RV-39. Borun vinnsluhluta frá 495 m í 2100 m*. National Energy Authority report. In Icelandic. OS-84109/JHD-47, 83 pp.
- Smárason, Ó.B., Tulinius, H., Tómasson, J., Thorsteinsson, Þ., Hermannsson, G., Guðmundsson, G. and Ágústsson, H. (1985a). *Reykjavík. Hola RV-37. Borun og rannsóknir*. National Energy Authority report. In Icelandic. OS-85109/JHD-63, 70 pp.
- Smárason, Ó.B., Tulinius, H., Tómasson, J., Thorsteinsson, Þ., Hermannsson, G. and Ágústsson, H. (1985b). *Reykjavík. Hola RV-36. Borun og rannsóknir*. National Energy Authority report. In Icelandic. OS-85113/JHD-66, 63 pp.
- Sæmundsson, K., Sigurgeirsson, M.Á., Hjartarson, Á., Kaldal, I., Kristinsson, S.G. and Víkingsson, S. (2016). *Geological map of SW-Iceland, 1:100.000* (2<sup>nd</sup> edition). Reykjavík: Iceland Geosurvey.
- Tómasson, J. (1988). *Elliðaársvæðið. Uppruni og eðli jarðhitans*. National Energy Authority report. In Icelandic. OS-88027/JHD-03, 67 pp.
- Tómasson, J. (1990). *The Elliðaár geothermal area. Nature and response to production*. National Energy Authority report.
- Tómasson, J. (1998a). *Jarðlög nágrannaholna Laugarnes- og Elliðaársvæðanna*. National Energy Authority short report. In Icelandic. JT-98-04, 2 pp.
- Tómasson, J. (1998b). *Megin jarðlagasýrur og vatnsæðar í borholum á Elliðaársvæði*. National Energy Authority short report. In Icelandic. JT-98/02, 4 pp.
- Tómasson, J., Thorsteinsson, Þ., Kristmannsdóttir, H. and Friðleifsson, I.B. (1977). *Höfuðborgarsvæði. Jarðhitarrannsóknir 1965-1973*. National Energy Authority report. In Icelandic. OSJHD-7703, 109 pp.
- Torfason, H. and Torfason, H. (1991). *Athugun á sprungum í Árbæ*. National Energy Authority report. In Icelandic. OS-91026/JHD-12, 8 pp. + maps.
- Tulinius, H., Smárason, Ó.B., Tómasson, J., Friðleifsson, I.B. and Hermannsson, G. (1986). *Hitastigulsboranir árið 1984 á höfuðborgarsvæði. Holur HS-14 til HS-22*. National Energy Authority report. In Icelandic. OS-86060/JHD-22, 38 pp.

## Appendix 1: List of data that has been imported in the 3D software from Seequent, Leapfrog Geothermal, that was used for both temperature and geological modelling

	Location in file system	Leapfrog file name	Description	Source	Source file name
Surface data - well locations	01_Topography	topography	Topography from National Land Survey of Iceland (Landmælingar Íslands). Resolution 25x25 m per pixel, extracted from a larger topography model	LMI open database	dem_IS50V.tif
	02_GIS_maps_pictures	loftmynd.png	Satellite picture of the Reykjavík area from the SPOT 5. Natural colours, original resolution is 2.5x2.5 m per pixel.	LMI and spot IMAGE	loftmynd.png
	02_GIS_maps_pictures	sprungur.shp	Additional fractures and faults in the Elliðaár area	Torfason and Torfason, 1990	sprungur.shp
	02_GIS_maps_pictures	sprungur_ISOR_100k.shp	Fractures and faults from a published geology map	Sæmundsson et al., 2016	sprungur_ISOR_100k.shp
	03_Well_Data	collar	Locations of well-heads	ISOR data base	collar.txt
	02_GIS_maps_pictures	jardlog-misgengi_vatnsrennsli_800m_JT1988	Lithology, fault, waterflow at 800 m depth	Tómasson, 1988	jardlog-misgengi_vatnsrennsli_800m_JT1988
	02_GIS_maps_pictures	ellidaarsvaedi_skipting_holur_JT1988	Map of production area, western area, eastern area, hydrological barriers and wells.	Tómasson, 1988	ellidaarsvaedi_skipting_holur_JT1988
Well data	03_Well_Data	survey	Well tracks	ISOR data base	survey.txt
	03_Well_Data	lithology_final	Stratigraphy in deep wells	Tómasson et al., 1977; Tómasson, 1988; Tómasson, 1998; Jónsson et al., 1998	lithology_final.txt
	03_Well_Data	berghiti_master	Formation temperature in wells	ISOR data base	berghiti_master.txt
	03_Well_Data	epidote	First appearance of epidote	Tómasson et al., 1977; Tómasson, 1988; Tómasson, 1998; Jónsson et al., 1998	epidote.txt
		Circulation_Losses	Circulation losses within the wells		
		Production_Stimulation	Production and stimulation		
	03_Well_Data	Master_1967 to Master_2020	All temperature logs from the wells from 1967 to 2020 ...	ISOR data base	Master_1967 to Master_2020
Cross-sections	05_Cross-sections	JT1988_R24_to_R33_temp_lith_flow	Cross-section - stratigraphy and water flow	Tómasson, 1988	hiti_jardlog_vatnsleidarar_rv24_til_rv33_JT1988
	05_Cross-sections	JTetal1977_R25_to_R29_lith	Stratigraphical cross section from R-25 to R-29	Tómasson et al., 1977	jardlagasnid_g25_til_g29_hofudborgarsvaedid
	05_Cross-sections	JTetal1977_K1_to_R27_lith	Stratigraphical cross section from K-01 to R-27	Tómasson et al., 1977	jardlagasnid_k1_til_g27_hofudborgarsvaedid
	05_Cross-sections	JTetal1977_K1_to_R33_lith	Stratigraphical cross section from K-01 to R-33	Tómasson et al., 1977	jardlagasnid_k1_til_rv33_hofudborgarsvaedid
	05_Cross-sections	JT1988_R25_to_R41_lith_temp_flow	Stratigraphy, temperature, waterflow, cross-section from R-25 to R-41	Tómasson, 1988	jardlog_jafnhitalinur_vatnsleidarar_rv25_til_rv41_JT1988
	05_Cross-sections	JT1988_R28_to_R36_lith_temp_flow	Stratigraphy, temperature, waterflow, cross-section from R-28 to R-36	Tómasson, 1988	jardlog_jafnhitalinur_vatnsleidarar_rv28_til_rv36_JT1988
	05_Cross-sections	JT1988_R31_to_R41_lith_temp_flow	Stratigraphy, temperature, waterflow, cross-section from R-31 to R-41	Tómasson, 1988	jardlog_jafnhitalinur_vatnsleidarar_rv31_til_rv41_JT1988
	05_Cross-sections	JT1988_R25_to_R36_lith	Stratigraphy from R-25 to R-36	Tómasson, 1988	jardlog_rv25_til_rv36_JT1988
	05_Cross-sections	JT1988_H20_to_R32_temp	Temperature cross section from H-20 to R-32	Tómasson, 1988	temperature_cs_h20_til_rv32_JT1988
	05_Cross-sections	JT1988_K1_to_H39_temp	Temperature cross section from K-01 to H-39	Tómasson, 1988	temperature_cs_k1_til_h39_JT1988
	05_Cross-sections	tomasson_1990_ellidaar_field_barriers	Elliðaárdalur geothermal field with hydrological barriers	Tómasson, 1990	tomasson_1990_ellidaar_field_barriers
	05_Cross-sections	JT1988_laugarnes_ellidaar_temp	Temperature cross section from Laugarnes to Elliðaár area	Tómasson, 1988	temperature_cs_laugarnes_ellidaar_JT1988

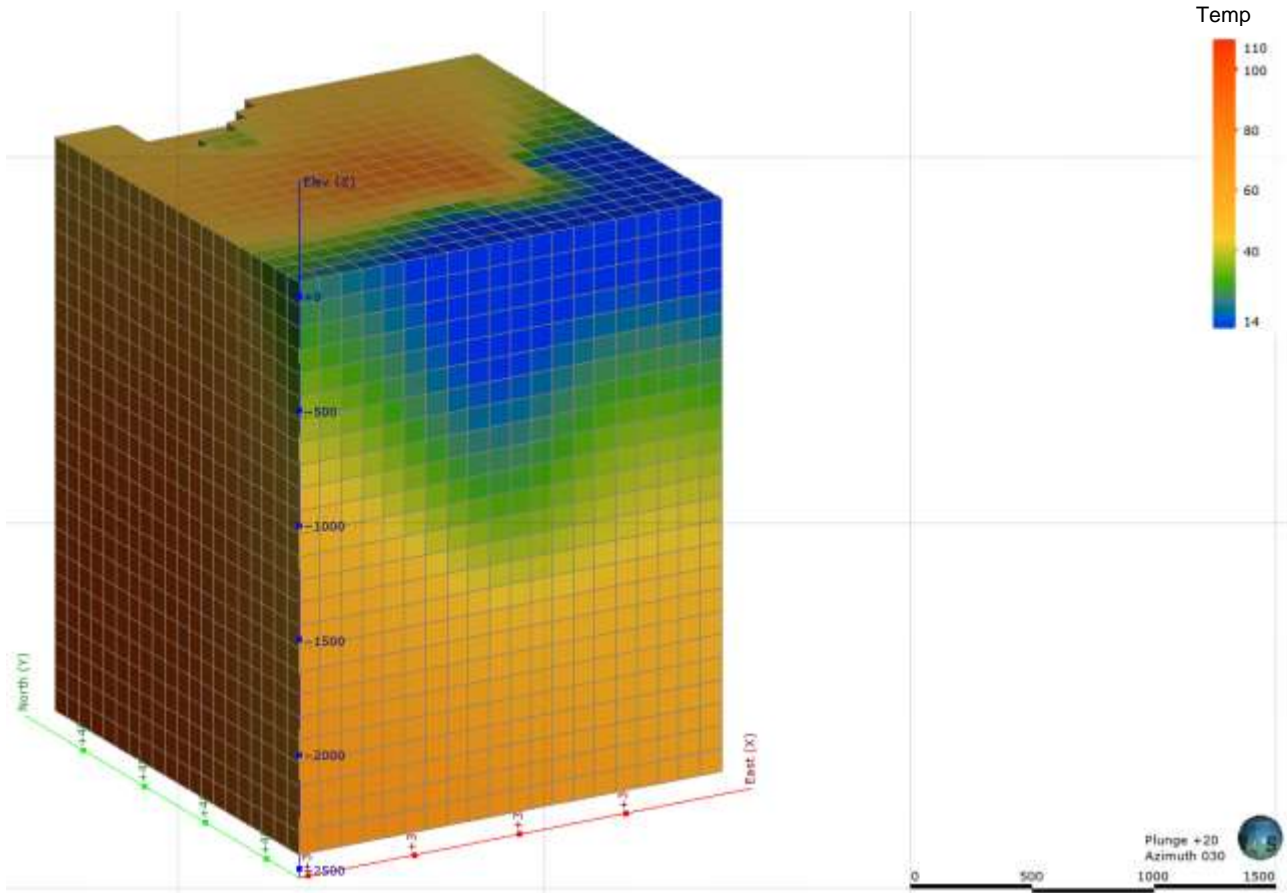
The RESULT project has been subsidized through the ERANET Cofund GEOTHERMICA (EC Project no. 731117), by RVO (the Netherlands), Rannis (Iceland) and GSI (Ireland)

## Appendix 2: System block model and isosurfaces



Northern view of a west-east slice of the lithological layers displaying the isosurfaces from 1968.

**3D modelling of lithology and temperature in the Elliðaárdalur low temperature geothermal area, Reykjavík, SW-Iceland**



*3D view of the block model (1968).*